Determination of the structure of mixed argon–xenon clusters using a finite-temperature, lattice-based Monte Carlo method

Daniel H. Robertson and Franklin B. Brown
Department of Chemistry and Supercomputer Computations Research Institute, Florida State University, Tallahassee, Florida 32306

I. Michael Navon
Department of Mathematics and Supercomputer Computations Research Institute, Florida State University, Tallahassee, Florida 32306

(Received 29 August 1988; accepted 18 November 1988)

The energy-optimized structures of all mixed Ar–Xe clusters containing 7, 13, and 19 atoms have been determined using a finite-temperature, lattice-based Monte Carlo procedure, which incorporates a highly efficient, memoryless, quasi-Newton-like conjugate gradient algorithm. This involves locating the global minima on the corresponding potential energy surfaces constructed from pairwise-additive Lennard-Jones potentials. For these systems, this optimization procedure has been found to be much more efficient than the more generally applicable simulated annealing method. Based on these energy-optimized structures, substitution sequences have been presented and discussed.

I. INTRODUCTION

Atomic and molecular clusters are involved in a number of phenomena including astrophysical processes, atmospheric reactions, nucleation, and catalysis. Although much of the theoretical and experimental research into the physical and chemical properties of clusters[1] has been driven by their potential catalytic properties, clusters are intrinsically important in any fundamental theory of matter as they form a natural bridge between atoms and molecules on the one hand, and liquids and solids on the other hand. Of the many interesting properties of clusters, some may be more appropriately described from a "molecular" viewpoint and others from a "bulk" viewpoint.

It has been known for a long time that the structures of small clusters in the gas phase generally differ from the packing structure of the substance in its crystalline state.[2] To understand the structures of rare-gas clusters (RGCs), various growth schemes have been proposed. The earliest models for describing the conformations of RGCs were developed by Werfelmeir[3] and were based on the principle of maximizing the coordination number of the atoms. These models yielded, for example, the equilateral triangle for 3 atoms, the tetrahedron for 4 atoms, the bitetrahedron for 5 atoms, the decahedron for 7 atoms, and the icosahedron for 13 atoms.[3] In general, the models for larger clusters were constructed by adding atoms to the faces and other symmetric positions of smaller clusters. This type of "building-up" procedure lead to the development of various growth schemes. For example, Hoare and Pal[4] constructed models of RGCs containing up to 60 atoms using growth schemes involving tetrahedral, pentagonal, and icosahedral symmetries. Energies were calculated for the models obtained from the different growth schemes using a pairwise-additive, Lennard-Jones potential. The model that gave the lowest energy for a cluster of a given number of atoms was assumed to represent the energy-optimized conformation. In all cases, the models based on the growth schemes gave lower energies than the corresponding model based on face-centered-cubic packing.

To aid in the interpretation of data from electron diffraction studies of RGCs, Farges *et al.*[5–7] used a growth scheme based on icosahedral structures. These investigators also employed molecular dynamics simulation methods with a pairwise-additive, Lennard-Jones potential, to determine the equilibrium structures of the clusters. Using this procedure, the structures of the clusters were allowed to relax from their purely polyicosahedral conformations. For the cluster containing 23 atoms, Farges *et al.*[6] located a new conformation that has a lower energy than that reported by Hoare and Pal.[4]

From a molecular viewpoint, the potential energy of the ground state of a cluster can be described by a hypersurface, which will be referred to as a potential energy surface (PES), of high dimensionality ($3N-6$, where N is the number of atoms in the cluster). The geometry of the cluster's most stable conformation is the geometry corresponding to the global minimum of the PES. A complication in locating these global minima arises from the fact that the PESs of clusters contain many local minima. In fact, the number of minima increases exponentially as the number of atoms increases. Hoare and McInnes[8] have reported that the number of minima discovered on PESs constructed from pairwise-additive, Lennard-Jones potentials, representing RGCs with 6, 7, 8, 9, 10, 11, 12, and 13 atoms are 2, 4, 8, 18, 57, 145, 366, and 988, respectively. Thus, to determine the energy-optimized conformations of these clusters, one must employ a method that will locate the global minimum on a PES and not become trapped in one of its many local minima.

One of the few optimization algorithms that is capable of locating the global minimum on a hypersurface is the simulated annealing (SA) method.[9] Recently, Wille[10] applied this method to determining the global minima of the PESs for a number of RGCs containing up to 25 atoms. The PESs were constructed from pairwise-additive, Lennard-Jones

 0021-9606/89/063221-09$02.10

potentials. In addition, Wille used a gradient optimizer to speed up the search for the minimum when the SA algorithm was at a low energy.[10] The advantage of using the SA method in determining energy-optimized conformations of clusters is that it is capable of locating a global minimum in the presence of multiple local minima. Using this method, Wille discovered new, energy-optimized conformations for RGCs with 23 and 25 atoms as compared with those reported by Hoare and Pal.[4]

Northby[11] has recently studied the structures of all Lennard-Jones, RGCs containing from 13 to 147 atoms. Using a lattice-based search followed by a local optimization procedure, Northby has reported optimized structures for all of these 135 clusters. The lattice structure that was used in the initial search for the energy-optimized geometry, was constructed from multilayer icosahedral structures. For many of these RGCs, the optimized structures determined by Northby have a significantly lower energy than previously reported structures.

Whereas, most of the previous studies of RGCs have focused on pure atomic clusters consisting of only one type of atom, we have investigated mixed RGCs that contain both argon and xenon atoms. For the pure RGCs, all of the two-body interactions are identical and the resulting structures often contain various symmetry elements. In the mixed clusters, many of these symmetry elements are missing. In the present study, we have investigated the most stable structures of mixed RGCs containing 7, 13, and 19 atoms. Pure RGCs of these sizes are particularly stable and have well defined geometric structures. Only a few studies of mixed RGCs have been reported in the literature. Scharf *et al.*[12] have investigated the dynamics of electronically and vibrationally excited states of $XeAr_{12}$, Xe_2Ar_{11}, $XeAr_{54}$, and Xe_2Ar_{53} RGCs. Recently, Boehmer and Peyerimhoff[13] have investigated the singly charged, cationic RGCs $[XeAr_{N-1}]^+$, $N = 3$–27 and compared their results to the mass spectra obtained by Ding and co-workers.[14]

The remainder of this paper is organized as follows: in Sec. II, we describe the computational methods that we used in this study. The results are presented in Sec. III and discussed in Sec. IV. Finally, the conclusions from this study are presented in Sec. V.

II. COMPUTATIONAL METHODS

As discussed in Sec. I, the problem of determining the energy-optimized structure of a cluster is equivalent to locating the global minimum of a PES. Most of the currently existing algorithms for optimization cannot distinguish between a global minimum and a local minimum. Thus, if one uses these methods for optimizing cluster structures, one has very little assurance that one has reached the global minimum because there are so many local minima.[4] In this section we describe the simulated annealing method along with a couple of variants that we have examined in developing a strategy for determining the energy-optimized structures of mixed RGCs. Finally, we present the finite-temperature, lattice-based Monte Carlo method and we describe the construction of the PESs that have been used to represent these mixed RGCs.

A. The simulated annealing method

One of the few optimization algorithms that can determine global minima is the simulated annealing method. This method was first applied to several discrete combinatorial optimization problems.[15] Subsequently, Vanderbilt and Louie[16] modified the SA method so that it can be applied to optimization problems that involve continuous variables.

The SA method is analogous to the thermal annealing of a crystal. During the annealing process, the crystal is heated to a relatively high temperature and then allowed to cool very slowly. At high temperatures, the particles in the crystal have enough thermal energy (kinetic energy) to overcome local conformational barriers and evolve into more stable structures. As the temperature is slowly lowered, the particles have less thermal energy and become more and more constrained, in their movement, by the local barriers. If the temperature is lowered slowly enough, the particles in the crystal become aligned and "organized" so as to minimize the energy. The configuration of this state corresponds to the global minimum on the PES representing this system. If however, the temperature is lowered too rapidly, the system may be quenched and become trapped in a metastable state, which corresponds to a local minimum on the PES.

Our implementation of the SA method for determining the energy-optimized structures of RGCs is very similar to Wille's[10] implementation. We employed the Metropolis algorithm.[17] Starting from a randomly chosen point on the PES of a cluster, which corresponds to a random cluster conformation, a step is taken along a random direction and the change in the potential energy ΔE is calculated. If ΔE is negative, the step is accepted. If ΔE is positive, the step is accepted with a probability determined by the Boltzmann factor P_B:

$$P_B = e^{-\Delta E/kT}, \tag{1}$$

where k is Boltzmann's constant and T is the temperature. In our implementation, we compare P_B with a random number and accept the step if P_B is greater than the random number. At high values of T, there is a greater probability of accepting steps for which ΔE is positive, i.e., accepting steps in an "uphill" direction. This allows the system to move across barriers into different regions of the PES at high temperatures. As the temperature is slowly lowered, there is a decreased probability of surmounting high barriers and the system slowly becomes localized until, at very low temperatures, it oscillates in the immediate vicinity of the global minimum.

As the system becomes localized in the vicinity of the global minimum, the SA method becomes inefficient in locating the exact position of the minimum. At this point, the SA method is allowing the system to take random walks in only one catchment region. In this situation, many other optimization algorithms will very quickly converge to the minimum. Wille[10] reported that he used a gradient optimizer when the SA algorithm reached low energies. In the present work, we have employed the memoryless, quasi-Newton-like conjugate-gradient method of Shanno[18,19] as implemented in the CONMIN program.[20] (See the Appendix.) We have used this local optimization algorithm for clusters containing as many as 55 atoms which involved op-

timizing 159 variables. In our cluster optimizations that employed the SA method in conjunction with the conjugate gradient method, less than 1% of the total computer time was spent in the CONMIN program.

This implementation of the SA method in conjunction with the conjugate gradient method is ideal when there is very little *a priori* information concerning the location of a global minima. This method treats all regions of the PES in a balanced manner. However, the SA method is relatively costly in terms of the number of evaluations of the potential energy that must be performed. In particular, one must perform long enough walks at each temperature so that representative regions of configuration space are sampled and one must employ a cooling schedule that does not allow for quenching. Finally, one must repeat the calculation several times, using different random numbers, to help insure that one has reached the global minimum. Thus, while the simulated annealing method is quite powerful, it is also quite costly.

B. Related optimization methods

Recently, Saunders[21] employed a Monte Carlo method which samples the minima of a PES by randomly stepping from minimum to minimum on the PES. This was accomplished by using a local optimizer to locate the nearest minimum, followed by applying a random displacement to all of the coordinates and then locating the nearest minimum to the new point. By monitoring the energies of all of the minima sampled, Saunders determined an upper bound on the global minimum. Assuming that one can reach the global minimum in a finite number of steps from any other minimum on the PES, this method will eventually yield the global minimum. Saunders used this method to determine optimized structures for various medium-sized cycloalkanes.[21]

Li and Scheraga[22] have used a similar method to determine the optimized folded structure for various proteins. Their method differs from Saunders' method in that Li and Scheraga only accept steps to new minima with a Boltzmann probability. Basically, these two methods are the same except that Saunders performs his walks using an infinite temperature so that $P_B = 1$ and all steps are accepted, while Li and Scheraga use a finite temperature for which $P_B < 1$ and some steps are rejected. These authors adjust the size of the random step and the temperature to achieve a step acceptance of about 50%.

C. The finite-temperature, lattice-based, Monte Carlo method

In the present study of mixed RGCs, we have developed a finite-temperature, lattice-based, Monte Carlo method. (This method will be denoted as FTLBMC.) This method is designed for studying these clusters that have an underlying structure (that of the pure RGC) which is relaxed or perturbed in the mixed RGC because of the presence of the two different types of atoms. For a cluster containing N atoms, we begin with the structure of the Ar_N cluster. Then we randomly substitute the appropriate number of Ar atoms with Xe atoms for the particular mixed cluster we are studying to form our initial structure S_0 of the mixed RGC. Using a local optimizer, we locate a minimum near S_0 and record its energy. Then returning to the structure S_0, we randomly interchange the position of one Ar atom with that of one Xe atom forming a new structure S_1. Again, using a local optimizer, we locate a minimum near S_1, record its energy, and calculate ΔE which is equal to the difference in energy between the minimum near S_1 and the minimum near S_0. If ΔE is negative, we accept S_1 and proceed to a new structure S_2, by randomly interchanging another Ar–Xe pair of atoms. If ΔE is positive, then we accept S_1 with a Boltzmann probability. If S_1 is not accepted, we return to S_0 and generate another structure S_1 by randomly interchanging another Ar–Xe pair. After the completion of a certain number of steps, an upper bound for the global minimum is given by the lowest-energy optimized structure.

We present performance characteristics of the FTLBMC method in Table I for two mixed RGCs. In particular, we show the performance of the method as a function of both the temperature that is used in calculating P_B and the number of steps taken in the random walks. The following general observations can be made. First of all, as the value of the temperature is increased, the percentage of steps that are accepted is increased and this is essentially independent of the number of steps in the walks. Obviously, in the limit as $T \to \infty$, the percentage of accepted steps approaches 100. Second, as the temperature is increased and as the number of steps per walk is increased, the number of different minima with different energies sampled by the FTLBMC method is increased. Third, the number of times the method samples the lowest-energy minimum increases with both an increase in the number of steps per walk and a decrease in the value of the temperature. This latter effect simply reflects the fact that with a lower temperature, there is a lower probability that higher-energy minima are sampled. Finally, it should be noted that for the $Ar_{13}Xe_6$ cluster, the global minimum is not reached for three runs at the higher temperatures. Of course, one cannot reduce the temperature too much, since the number of accepted steps will become too small, thereby limiting the regions of configuration space that are sampled. In the limit at $T \to 0$ K, the method will only step to minima with lower energies which may prohibit the method from locating the global minimum. Based on our experience using this method with these systems, we have found that using a reduced temperature value of 0.5 (60 K for these studies) is reasonable as approximately 50% of the steps are accepted.

Furthermore, we have compared the performance of the FTLBMC method for mixed RGCs containing N atoms, in which the initial underlying structure is taken to be either the energy-optimized Ar_N or Xe_N structures. There is essentially no difference in performance between using either of these two structures as the underlying reference structure and so we have used the Ar_N energy-optimized structure in the present calculations.

As in the SA method, one should run the FTLBMC method several times using different sets of random numbers to increase the probability that the lowest-energy minimum sampled is, in fact, the desired global minimum. Nonetheless, the FTLBMC method is significantly faster than the SA

TABLE I. Performance characteristics of the finite-temperature, lattice-based Monte Carlo optimization method as a function of the number of steps and the temperature. The reduced energies of the optimized structures of Ar_7Xe_6 and $Ar_{13}Xe_6$ are -63.7979 and -98.0988, respectively.

Cluster	$\tilde{T}$[a]	NSTEPS[b]	NDES[c]	NTLES[d]	PSA[e]	$\tilde{E}_{LE}$[f]
Ar_7Xe_6	0.1	1000	13	477	17	−63.7979
		2000	15	1046	13	−63.7979
	0.5	1000	23	101	64	−63.7979
		2000	18	202	64	−63.7979
	1.0	1000	27	47	78	−63.7979
		2000	26	100	77	−63.7979
	10	1000	31	15	96	−63.7979
		2000	31	41	96	−63.7979
$Ar_{13}Xe_6$	0.1	1000	15	835	5	−98.0988
		2000	17	1721	3	−98.0988
	0.5	1000	180	3	42	−98.0988
		2000	282	14	45	−98.0988
	1.0	1000	376	7	63	−97.6118
		2000	509	4	64	−98.0988
	10	1000	673	2	96	−97.7750
		2000	1036	1	94	−97.3937

[a] Reduced temperature: $\tilde{T} \equiv [T(\mathrm{K})/120\ \mathrm{K}]$.
[b] NSTEPS ≡ number of steps during optimization walk.
[c] NDES ≡ number of minima with different energies that were sampled.
[d] NTLES ≡ number of times the minimum with the lowest energy was sampled.
[e] PSA ≡ percentage of steps accepted.
[f] $\tilde{E}_{LE}$ ≡ lowest energy, in reduced units, of any minimum sampled. $\tilde{E} \equiv E/[(120\ \mathrm{K})(k)]$ where k is Boltzmann's constant.

method. While the SA method is a viable alternative for determining optimized structures for pure RGCs, it requires significantly longer runs for optimizing mixed RGCs. This is primarily because it takes many concerted moves of specific atoms to produce an interchange in position of an Ar–Xe pair of atoms. This type of interchange is not required for optimizing pure RGCs. As examples of the difference in timings between the SA method and the FTLBMC method, consider the optimization of the Ar_7Xe_6 and $Ar_{13}Xe_6$ clusters. They required 55 and 398 min of VAX 8700 CPU time, respectively, using the SA method and only 15 and 51 min, respectively, using the FTLBMC method. Thus, for determining the energy-optimized structures of mixed RGCs that are strongly related to a particularly stable pure RGC, the FTLBMC method appears to be quite efficient.

D. The potential energy surfaces

The PESs that we used to model these systems consisted of pairwise-additive, Lennard-Jones potentials. The form of the Lennard-Jones potential that we used for a two-body interaction was

$$V_{ij}(r_{ij}) = 4\epsilon\left[\left(\frac{\sigma}{r_{ij}}\right)^{12} - \left(\frac{\sigma}{r_{ij}}\right)^{6}\right], \tag{2}$$

where the r_{ij} is the distance between atoms i and j. The values for the parameters ϵ and σ for the three different types of rare-gas atom interactions are given in Table II.

TABLE II. Parameters that have been used in the two-body, Lennard-Jones potentials describing the interaction between two rare-gas atoms. These parameters were taken from Ref. 12.

Interaction	σ (Å)	ϵ/k (K)	$\tilde{\epsilon}$[a]
Ar–Ar	3.40	120.0	1.0000
Ar–Xe	3.65	177.6	1.4800
Xe–Xe	4.10	222.3	1.8525

[a] $\tilde{\epsilon} \equiv \epsilon/[(120\ \mathrm{K})(k)]$ where k is Boltzmann's constant.

III. RESULTS

In this investigation we have determined the energy-optimized structures for all of the mixed Ar–Xe clusters containing 7, 13, and 19 atoms. We chose to examine these particular clusters because the corresponding pure RGCs are quite stable and have high symmetries. In particular, 7 has pentagonal symmetry, 13 has icosahedral symmetry, and 19 has biicosahedral symmetry. Thus, these clusters are ideal systems to investigate using the FTLBMC method.

We present the lowest energies obtained for all of these mixed clusters in Tables III, IV, and V. These energies represent an upper bound on the energy of the global minima for these systems and although there is no guarantee that we have found the global minimum for each of these systems, there is a high probability that we have indeed located it.

TABLE III. Energies of the optimized structures of the $Ar_{7-n}Xe_n$ clusters where $0 \leqslant n \leqslant 7$.

No. of Ar atoms	No. of Xe atoms	$\tilde{E}$[a]
7	0	−16.5054
6	1	−19.2622
5	2	−22.0179
4	3	−23.7468
3	4	−25.5027
2	5	−27.2248
1	6	−28.8997
0	7	−30.5762

[a] $\tilde{E}$ is the energy in reduced units.

TABLE IV. Energies of the optimized structures of the $Ar_{13-n}Xe_n$ clusters where $0 \leqslant n \leqslant 13$.

No. of Ar. atoms	No. of Xe atoms	$\tilde{E}$ [a]
13	0	−44.3268
12	1	−47.6968
11	2	−51.1213
10	3	−54.5957
9	4	−57.8542
8	5	−60.7363
7	6	−63.7979
6	7	−66.5918
5	8	−69.0209
4	9	−71.6010
3	10	−74.0184
2	11	−76.2746
1	12	−78.7008
0	13	−82.1154

[a] $\tilde{E}$ is the energy in reduced units.

This confidence comes from performing the FTLBMC calculations several times and never sampling a point on the corresonding PES with a lower energy.

In Figs. 1, 2, and 3 we schematically present the order of substitution of Ar atoms with Xe atoms for each cluster size. In most cases, the actual mixed RGCs have a lower symmetry than is depicted in these figures, because we have treated the Ar and Xe atoms alike in these schematic diagrams so that the substitution sequences are most clearly displayed. Of course, in our calculations, these effects entered via the different sets of parameters that were used in the Lennard-Jones potentials. In Fig. 4, we illustrate the asymmetric structures of the Ar_3Xe_4 and Ar_2Xe_5 clusters.

Finally, in Fig. 5, we present a plot of the lowering of the energy that occurs with each successive substitution of an Ar atom with a Xe atom. For a given cluster size, the sum of each of these energies gives the difference between the energies of the pure Ar_N and Xe_N clusters.

TABLE V. Energies of the optimized structures of the $Ar_{19-n}Xe_n$ clusters where $0 \leqslant n \leqslant 19$.

No. of Ar atoms	No. of Xe atoms	$\tilde{E}$ [a]
19	0	−72.6598
18	1	−77.2961
17	2	−81.9063
16	3	−86.3261
15	4	−90.4299
14	5	−94.3788
13	6	−98.0988
12	7	−101.8070
11	8	−104.5712
10	9	−107.5304
9	10	−110.2436
8	11	−113.0753
7	12	−115.6808
6	13	−118.2847
5	14	−120.7866
4	15	−123.7816
3	16	−126.5652
2	17	−129.1322
1	18	−131.8380
0	19	−134.6023

[a] $\tilde{E}$ is the energy in reduced units.

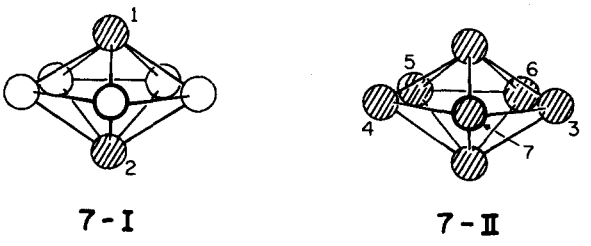

FIG. 1. Schematic representation of the substitution sequence for Ar–Xe clusters containing seven atoms. The shaded and open circles represent Xe and Ar atoms, respectively.

IV. DISCUSSION

From an analysis of the geometries of the energy-optimized structures of these various mixed RGCs, it is apparent that they all retain the gross structure of the underlying pure RGC. This was confirmed by using the SA method to determine the global minima for several of these clusters. In all cases that we checked, the "unbiased" nonlattice-based SA method gave the same optimized structure. Thus the energy-optimized structures of these mixed RGCs are perturbed or "relaxed" forms of the corresponding pure RGC structures.

The next interesting aspect of this investigation involves developing an understanding of the substitution sequence that occurs in these clusters. Of course, in an actual experimental situation, it may not be the case that a mixed RGC would be formed by a sequential substitution of Ar atoms with Xe atoms. Nonetheless, the concept of sequential substitution provides a method for organizing the various mixed RGCs for a given cluster size in much the same way that various growth schemes for the pure RGCs have been used.

In trying to understand the substitution sequences for these RGCs, it is important to keep in mind the relative well

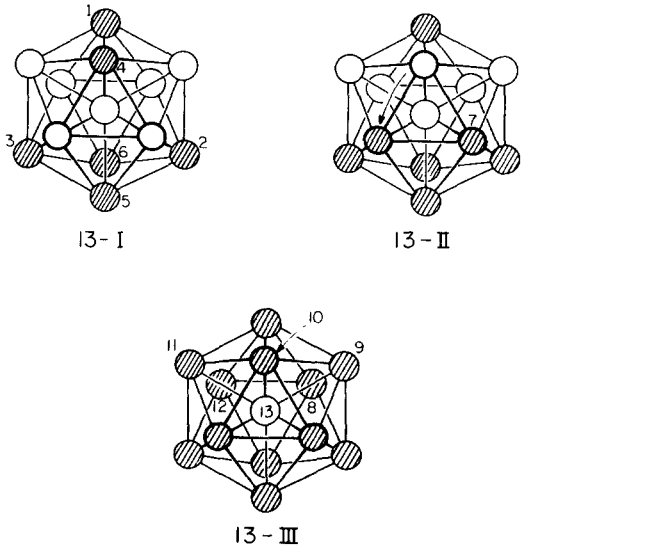

FIG. 2. Schematic representation of the substitution sequence for Ar–Xe clusters containing 13 atoms. The shaded and open circles represent Xe and Ar atoms, respectively.

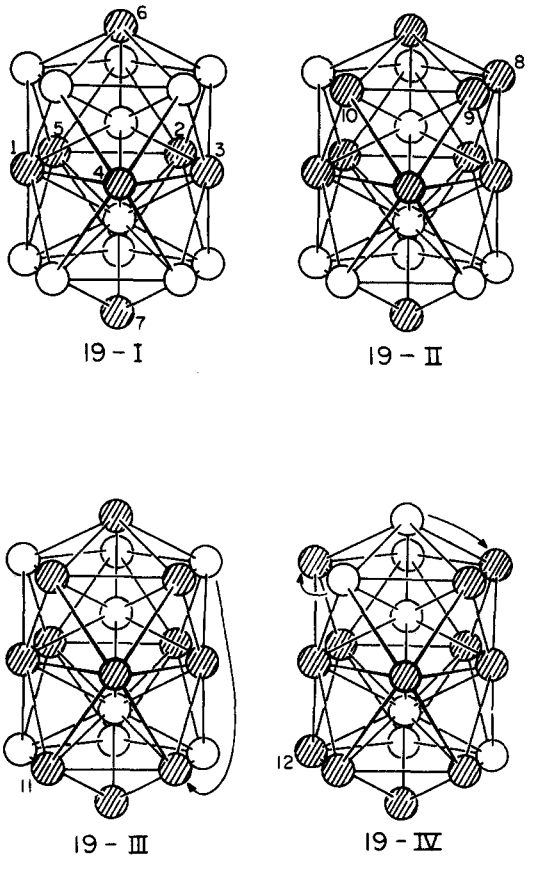

FIG. 3. Schematic representation of the substitution sequence for Ar–Xe clusters containing 19 atoms. The shaded and open circles represent Xe and Ar atoms, respectively.

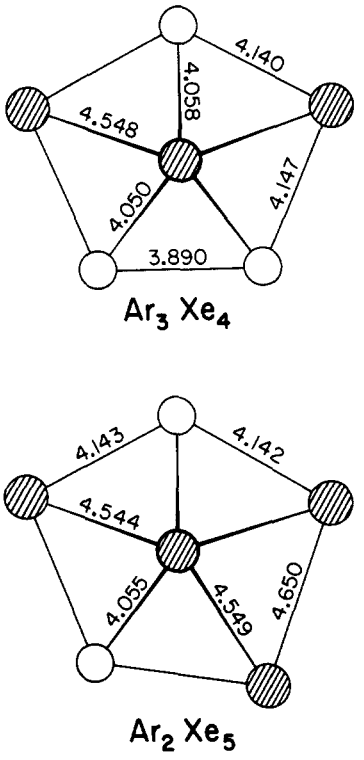

FIG. 4. The energy-optimized structures of the Ar_3Xe_4 and Ar_2Xe_5 mixed RGCs. As before, the shaded and open circles represent Xe and Ar atoms, respectively. The perspective is directly along the axis containing the apex atoms—there is an additional Xe atom hidden directly below the central Xe atom.

depths of the three Lennard-Jones interaction potentials. The strongest attractive interaction is the Xe–Xe interaction while the weakest is the Ar–Ar interaction. In the crudest model, when there are more Ar atoms than Xe atoms, one wants to maximize the number of Ar–Xe nearest-neighbor interactions and minimize the number of Ar–Ar nearest-neighbor interactions. However, when there are more Xe atoms than Ar atoms, one wants to maximize the number of Xe–Xe nearest-neighbor interactions. Of course, all of this is mediated by the fact that these strong attractive interactions occur at different interatomic distances for the three differ-

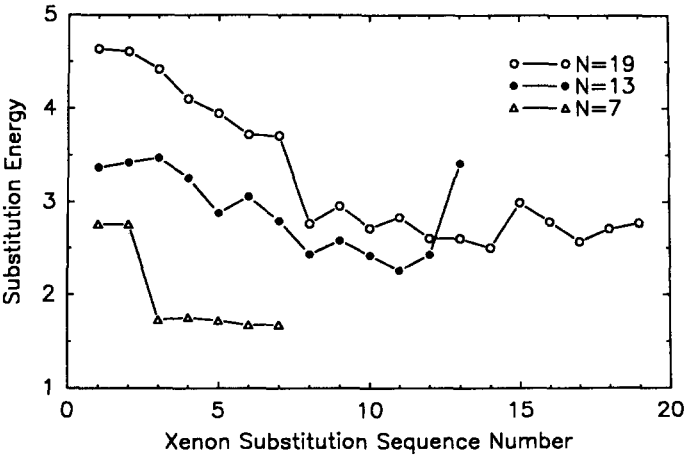

FIG. 5. Plots of the energy lowering for the substitution of each Xe atom into the mixed RGCs containing 7, 13, and 19 atoms. The energy lowering is given in reduced units. (See Table I).

ent two-body potentials. Thus, for the larger mixed RGCs, the most intuitive structure is not always the energy-optimized structure. (For these "counterintuitive" structures, we have always investigated the minima in the region of the "intuitive" structures and found that the latter had higher energies.) We now discuss the substitution sequence for each cluster size separately. (In describing the substitution sequence for a particular mixed RGC, it should be noted that sometimes the structure will have symmetry-equivalent structures. In these cases we have simply chosen the structure that most clearly depicts the substitution sequence.)

A. RGCs containing seven atoms

As mentioned before, the Ar_7 and Xe_7 clusters have pentagonal structures with five atoms in a plane forming a regular pentagon structure and two apex atoms, one above and one below the plane. (This structure is schematically presented in Fig. 1.) Starting from the Ar_7 structure, the first two Xe substitutions occur at the two apex positions (7-I). The third Xe atom substitutes into any of the planar positions. The fourth and fifth Xe atoms substitute into the pentagonal ring to positions that maximize the number of nearest-neighbor Ar–Xe interactions while minimizing the number of Xe–Xe nearest-neighbor interactions (7-II).

In examining Fig. 5, one can see that the greatest energy was gained from first two substitutions into the two apex positions. The energy gained from substitution into the axial positions was almost constant. Thus, the Ar_6Xe and Ar_5Xe_2 are particularly stable as they maximize the number of Ar–Xe interactions and minimize the number of Ar–Ar interactions.

In Fig. 4, we present the structures of the Ar_3Xe_4 and Ar_2Xe_5. In this figure, the distortion from the corresponding pure (symmetric) Ar_7 structure is apparent with the Ar–Ar interatomic distances being shorter than the Ar–Xe distances which are shorter than the Xe–Xe distances.

B. RGCs containing 13 atoms

The Ar_{13} and Xe_{13} clusters have icosahedral symmetry. Their structure can be considered to be composed of two clusters containing seven atoms that are positioned directly above each other and share an apex atom. Furthermore, the pentagonal rings are rotated by $\pi/5$ rad relative to each other. This icosahedron has 12 atoms around a central atom.

The substitution sequence is schematically depicted in Fig. 2. Structure 13-I shows the first six substitutions. The first substitution occurs at an apex position, followed by two substitutions on the lower pentagonal ring. The fourth substitution occurs on the top pentagonal ring, followed by a substitution of the bottom apex atom, and another atom in the lower pentagonal ring. At this point there is a restructuring of the substitution sequence to complete the bottom pentagonal ring (13-II). The atom substituted in the top pentagonal ring moves to the bottom pentagonal ring and the seventh substitution completes this lower pentagonal ring. The remainder of the substitution sequence occurs by filling up the upper pentagonal ring followed by substitution of the central atom (13-III). Presumably, the central atom is the last to be substituted because of the high energy associated with stretching the Ar–Ar interactions to allow the much larger Xe atom to occupy this central site.

In examining the relative energetics of the substitution sequence as depicted in the appropriate plot in Fig. 5, one observes that the substitution energies are relatively smooth with the only sharp feature occuring with the substitution of the central (last remaining) atom. This last substitution significantly lowers the energy because at this point, the system is no longer perturbed from an optimal Xe_{13} structure. The most stable structures of these mixed RGCs, with respect to substitution, are $Ar_{10}Xe_3$, Ar_7Xe_6, and Ar_4Xe_9.

C. RGCs containing 19 atoms

The pure RGC containing 19 atoms is made up of two vertically interpenetrating icosahedra that share the two interior atoms and the central pentagonal ring of atoms. The substitution sequence for this cluster is schematically shown in Fig. 3. The central pentagonal ring of Ar atoms are substituted first, followed by substitutions of the top and bottom apex atoms (19-I). Three atoms in either the top pentagonal ring or the bottom pentagonal ring are substituted next (19-II). This is followed by a restructuring in which one Xe atom from the partly filled pentagonal set moves to the opposite pentagonal ring followed by a substitution at a site on the latter pentagonal ring (19-III). At this point, both the bottom and top pentagonal rings contain two Xe atoms. The next substitution involves moving an apex Xe atom to the nearest pentagonal ring and substituting a Xe on the opposite pentagonal ring (19-IV). At this point, the upper and lower pentagonal rings each contain three Xe atoms. The 13th Xe atom substitutes at the unsubstituted apex position (19-V). The next substitution occurs at one of the pentagonal rings simultaneously with an Xe atom from the opposite apex substituting into this ring to complete its substitution (19-VI). Then the central (interior) atom on the almost completed icosahedron is substituted along with the replacement of a Xe on the opposite apex position (19-VII). Finally the partially unsubstituted pentagonal ring is completely substituted (19-VIII). The last atom to be substituted is the second interior atom.

Although this sequence is more complicated than those described previously for the 7- and 13-atom RGCs, they have several features that are common. For example, the interior atom inside an icosahedral structure is only added after the outside framework has been substituted. These clusters tend to maximize their symmetry which in some cases is manifested by favoring the completion of pentagonal rings. Of course, there are exceptions to these general rules and in cases where counterintuitive structures were found, we examined the more intuitive structure and found in all cases that the latter structure had a higher energy than the former structure—although, in most cases the energy difference, while significant, was not large.

Figure 5 shows that there is a significant decrease in the substitution energy in going from $Ar_{12}Xe_7$ to $Ar_{11}Xe_8$. The former structure has maximized the number of Ar–Xe interactions and strain begins to enter the system with the substi-

tution of the eighth Xe atom. Also, note that the substitution of the interior Xe atom greatly lowers the energy as the outer framework allows for this substitution which increases the number of Xe–Xe interactions.

Alternatively, one can view this substitution sequence, not as a single scheme with atomic rearrangements between the clusters, but as a composite of several different schemes in which the scheme associated with the energy-optimized structure differs from one cluster to the next. When the ratio of Ar atoms to Xe atoms is close to unity, the energies of these difference schemes are very similar and therefore, no one substitution scheme predominates. For example, from Fig. 3, it can be seen that Ar_8Xe_{11} (19-III) is an $Ar_{10}Xe_9$ (19-II) with two Xe atoms substituted into the lower pentagonal ring. Similarly, Ar_6Xe_{13} (19-V) can be thought of as either an Ar_9Xe_{10} (19-II) with three Xe atoms substituted into the lower pentagonal ring or an Ar_8Xe_{11} (19-III) with two Xe atoms substituted, one in the upper ring and one in the lower ring. Likewise, Ar_5Xe_{14} (19-VI) is an Ar_7Xe_{12} (19-IV) with two Xe atoms substituted to complete the lower pentagonal ring. In examining Fig. 5, one can see that the substitution energies between $n = 8$ and $n = 14$ for the clusters containing 19 atoms are relatively constant—this being the region where the several substitution schemes overlap. Thus, one may view the overall substitution scheme, not as one, single-atom substitution sequence with atomic rearrangements between structures, but as a composite of several, near-degenerate, single-atom substitution sequences without atomic rearrangements.

V. CONCLUSIONS

In this paper, we have presented an investigation designed to determine the energy-optimized structures of RGCs containing both Ar and Xe atoms. To efficiently perform these optimization calculations, we have developed the finite-temperature, lattice-based Monte Carlo procedure that is related to the descretized simulated annealing method. As part of the FTLBMC algorithm, we have employed a highly efficient, local conjugate-gradient optimizer. We have examined the three families of clusters containing 7, 13, and 19 atoms.

We have described the structures of the mixed RGCs by considering substitution sequences and the corresponding substitution energies. By analyzing the substitution energy sequence, one can determine which substituted structures are more stable, relative to further substitution, than others. Most of these structures maximize the symmetry of the cluster which often is manifested by forming completely substituted pentagonal rings, and either maximizing the number of nearest-neighbor Ar–Xe interactions when there is a majority of Ar atoms in the cluster or nearest-neighbor Xe–Xe interactions when there is a majority of Xe atoms in the structure.

Further work on this project will involve using more accurate two-body potentials to construct the PESs of the RGCs. Additionally, we will investigate the performance of the FTLBMC method for mixed RGCs whose structures may not be as strongly linked to the corresponding, pure RGC as the ones in this study.

ACKNOWLEDGMENTS

This work was partially supported by the U. S. Department of Energy through Contract No. DE-FC05-85ER250000. This research was also supported in part by the Florida State University through time granted on its Cyber 205 supercomputer.

APPENDIX

The CONMIN program proposed by Shanno and Phua[20] finds the local minimizer of a nonlinear function of n variables, $f(\mathbf{x})$, where

$$\mathbf{x} = (x_1,\ldots,x_n)^T, \quad n \geqslant 1 \tag{A1}$$

can be any real numbers. This program incorporates two nonlinear optimization methods, i.e., a conjugate-gradient algorithm and a quasi-Newton algorithm, with the choice of the method being left to the user.

The conjugate-gradient algorithm in CONMIN is the Beale restarted memoryless variable metric algorithm documented in Shanno.[18,19] This method requires approximately $7n$ single/double precision words of working space to be provided by the user.

The quasi-Newton method is the Broyden–Fletcher–Goldfarb–Shanno (BFGS) algorithm with initial scaling documented in Shanno and Phua.[23] This method requires approximately $n^2/2 + 11n/2$ double precision words of working storage.

For solving large-scale nonlinear optimization problems, memory considerations generally mandate using the conjugate-gradient algorithm, i.e., we used only the conjugate gradient option of CONMIN

The performance of this conjugate-gradient code can be significantly improved by careful implementation on supercomputers when solving large-scale optimization problems.

Algorithmic description of the Shanno–Phua[20] conjugate-gradient method.

(i) Initialization:

$$\begin{aligned} &\text{Choose } x_0,\ \epsilon,\ H_0 = \mathrm{I} \text{ and set } k = 0,\\ &\text{compute} \quad f_k = f(\mathbf{x}_k),\\ &\qquad\qquad g_k = g(\mathbf{x}_k), \quad \text{i.e., the gradient of } f,\\ &\qquad\qquad s_k = -g_k,\\ &\text{and} \qquad\qquad s_k^T g_k. \end{aligned} \tag{A2}$$

(ii) Linear search procedure:

In this step, we perform the inexact linear search procedure proposed by Shanno and Phua[23] with some modifications. The basic linear search uses Davidon's cubic interpolation to find a step length α_k which satisfies the following two conditions:

$$f(\mathbf{x}_k + \alpha_k s_k) < f(\mathbf{x}_k) + 0.0001\alpha_k s_k^T g_k, \tag{A3}$$

$$|s_k^T g(\mathbf{x}_k + \alpha_k s_k) s_k^T g_k| < 0.9. \tag{A4}$$

(iii) Test for convergence:

Set $\mathbf{x}_{k+1}=\mathbf{x}_k+\alpha_k s_k$,

$$f_{k+1}=f(\mathbf{x}_{k+1}),$$

$$g_{k+1}=g(\mathbf{x}_{k+1}), \tag{A5}$$

$$p_k=\mathbf{x}_{k+1}-\mathbf{x}_k,$$

$$y_k=g_{k+1}-g_k.$$

If $\|g_{k+1}\|\leqslant\epsilon\max(1,\|\mathbf{x}_{k+1}\|)$ then stop. Else proceed to step (iv).

(iv) Perform the Beale restart according to Powell's criterion:

If the following criterion suggested by Powell[24] holds, then perform the Beale[25] restart procedure described in this step. Otherwise proceed to step (v). Powell's[24] restart criteria are the following:

(a) The iteration k is a multiple of n.

(b) $|g_{k+1}^T g_k|\geqslant\|g_{k+1}\|^2$. (A6)

If either one of the above two conditions holds, then perform the following: Compute the new search direction s_{k+1} by

$$s_{k+1}=-\gamma g_{k+1}-\left[\left(1+\gamma\frac{y_k^T y_k}{p_k^T y_k}\right)\frac{p_k^T g_{k+1}}{p_k^T y_k}-\gamma\frac{y_k^T g_{k+1}}{p_k^T y_k}\right]p_k+\frac{\gamma p_k^T g_{k+1}}{p_k^T y_k}y_k, \tag{A7}$$

where

$$\gamma=\frac{p_k^T y_k}{y_k^T y_k}. \tag{A8}$$

Set

$p_t=s_k$, $y_t=y_k$, and go to step (ii).

(v) Compute the new search direction by the two-step memoryless BFGS formula:

This is a nonrestart step in which we compute the new search direction by using the two-step memoryless BFGS scheme as suggested by Shanno.[18] That is, we compute s_{k+1} by

$$s_{k+1}=-\hat{H}_k g_{k+1}+\frac{p_k^T g_{k+1}}{p_k^T y_k}\hat{H}_k y_k-\left[\left(1+\frac{y_k^T\hat{H}_k y_k p_k^T g_{k+1}}{p_k^T y_k\, p_k^T y_k}-\frac{y_k^T\hat{H}_k g_{k+1}}{p_k^T y_k}\right)\right]p_k. \tag{A9}$$

Here $\hat{H}$ is an approximation to the inverse Hessian and the vectors $\hat{H}_k g_{k+1}$ and $H_k y_k$ are defined by

$$\hat{H}_k g_{k+1}=\frac{p_k^T y_t}{y_t^T y_t}g_{k+1}-\frac{p_t^T g_{k+1}}{y_t^T y_t}y_t+\left(\frac{p_t^T g_{k+1}}{p_t^T y_t}-\frac{y_t g_{k+1}}{P_t^T y_t}\right)p_t \tag{A10}$$

and

$$\hat{H}_k y_k=\frac{p_t^T y_t}{y_t^T y_t}y_k-\frac{p_t^T y_k}{y_t^T y_t}y_t+\left(2\frac{p_t^T y_k}{p_t^T y_t}-\frac{y_t y_k}{y_t^T y_t}\right)p_t. \tag{A11}$$

As suggested by Fletcher,[25] the search vector s_{k+1} is scaled by

$$\hat{s}_{k+1}=[2(f_{k+1}-f_k)/g_{k+1}^T S_{k+1}]s_{k+1}. \tag{A12}$$

Go to step (ii).

[1]Surf. Sci. **156** (1985), edited by K. H. Benneman and J. Koutecky.
[2]L. H. Germer, Phys. Rev. **56**, 58 (1939).
[3]W. Werfelmeir, Z. Phys. **107**, 332 (1937).
[4]M. R. Hoare and P. Pal, Adv. Phys. **20**, 161 (1971).
[5]J. Farges, M. F. De Feraudy, B. Raoult, and G. Torchet, J. Chem. Phys. **78**, 5067 (1983).
[6]J. Farges, M. F. De Feraudy, B. Raoult, and G. Torchet, Surf. Sci. **156**, 370 (1985).
[7]J. Farges, M. F. De Feraudy, B. Raoult, and G. Torchet, J. Chem. Phys. **84**, 3491 (1986).
[8]M. R. Hoare and J. A. McInnes, Adv. Phys. **32**, 791 (1983).
[9]S. Kirkpatrick, C. D. Gelatt, Jr., and M. P. Vecchi, Science **220**, 671 (1983).
[10]L. T. Wille, Chem. Phys. Lett. **133**, 405 (1987).
[11]J. A. Northby, J. Chem. Phys. **87**, 6166 (1987).
[12]D. Scharf, J. Jortner, and U. Landman, J. Chem. Phys. **88**, 4273 (1988).
[13]H. U. Boehmer and S. D. Peyerimhoff, Z. Phys. D **8**, 91 (1988).
[14]H. U. Boehmer, G. Gantefor, M. Gilles, R. Hector, E. Holub-Krappe, and E. Ding in DFG-Schwerpunktprogramm "Physik anorganischer Cluster," 1. Arbeitsbericht uber die Forderungsperiode from April 1, 1985 to March 31, 1987.
[15]Perhaps the most famous of these types of problems is the traveling salesman problem which can be described as follows: Given a list of cities and an equation for calcuating the cost of traveling between any two cities, one must determine the route for the salesman that will pass through each city once, return to the starting point, and have the lowest total cost. This problem belongs to the NP-complete (nondeterministic polynomial time complete) class of problems.
[16]D. Vanderbilt and S. G. Louie, J. Comp. Phys. **56**, 259 (1984).
[17]N. Metropolis, A. W. Rosenbluth, M. N. Rosenbluth, A. H. Teller, and E. Teller, J. Chem. Phys. **21**, 1087 (1953).
[18]D. F. Shanno, Math. Oper. Res. **3**, 244 (1978).
[19]D. F. Shanno, SIAM J. Numer. Anal. **15**, 1247 (1978).
[20]D. F. Shanno and K. H. Phua, ACM Trans. Math. Software **6**, 618 (1980).
[21]M. Saunders, J. Am. Chem. Soc. **109**, 3150 (1987).
[22]Z. Li and H. A. Scheraga, Proc. Natl. Acad. Sci. USA **84**, 6611 (1987).
[23]D. F. Shanno and K. H. Phua, Math. Prog. **14**, 149 (1976).
[24]M. J. D. Powell, Math. Programm. **12**, 241 (1977).
[25]E. M. L. Beale, *Numerical Methods for Nonlinear Optimization* (Academic, London, 1972), p. 391.
[26]R. Fletcher, in *Numerical Methods for Unconstrained Minimization*, edited by W. Murray (Academic, London, 1972), p. 144.